Journal of Solid State Chemistry 247 (2017) 13–19

Contents lists available at ScienceDirect

Journal of Solid State Chemistry

journal homepage: www.elsevier.com/locate/jssc

Morin-like spin canting in the magnetic $CaFe_5O_7$ ferrite: A combined neutron and Mössbauer study

C. Delacotte[a], Y. Bréard[a], V. Caignaert[a], V. Hardy[a], J.M. Greneche[b], S. Hébert[a], E. Suard[c], D. Pelloquin[a,*]

[a] Laboratoire CRISMAT ENSICAEN UMR CNRS 6508, 6 Boulevard du Maréchal Juin, 14050 Caen Cedex 04, France
[b] Institut des Molécules et Matériaux du Mans, IMMM UMR CNRS 6283, Avenue Olivier Messiaen, 72085 Le Mans, France
[c] Institut Laue-Langevin, 71 avenue des Martyrs, 38042 Grenoble Cedex 9, France

ARTICLE INFO

Keywords:
Magnetic structure
Neutron diffraction
Mössbauer spectroscopy

ABSTRACT

Magnetic structure of $CaFe_5O_7$ ferrite has been studied jointly from neutron powder diffraction data and spectroscopic Mössbauer measurements in the thermal range from 5 to 500 K. This coupled work highlights three distinct magnetic domains around two specific temperatures: T_M=125 K and T_N=360 K. The latter corroborates the structural monoclinic-orthorhombic transition previously reported by transmission electron microscopy techniques and X-ray thermodiffractometry. Complementary heat capacity measurements have confirmed this first order transition with a sharp peak at 360 K. Interestingly, this large study has revealed a second magnetic transition associated to a spin rotation at 125 K similar to this one reported by Morin in α-Fe_2O_3 hematite at T_M=260 K.

1. Introduction

Iron oxides and related iron rich materials focus large attentions due to numerous and complex structural properties reported. A large part of this richness results from some oxygen non stoichiometry effects or intergrowth mechanisms which can generate potentially several crystallographic iron sites in the structure. Such a structural multiplicity offers the possibility to have different valence states or electronic configurations for iron species inside the structure like exemplified by the $Fe_{1-x}O$ [1] oxides or the hexaferrite-type compounds [2] and more recently by $CaBaFe_4O_7$[3]. Assuming these mixed state valences, some strongly correlated electron systems are thus obtained which lead to fascinating magnetic – transport properties. The magnetite Fe_3O_4 spinel like structure is a well-known example of a mixed valent Fe^{II}/Fe^{III} ferrimagnetic oxide (T_N=860 K). Apart from its magnetic behavior, its fame is the occurrence of a reversible structural transition at around 120 K –so called Verwey transition- associated to an ordering of the ionic charge state [4,5]. Among the different iron based oxide systems, the Ca-Fe-O one and especially the intergrowth $(CaFe_2O_4)(FeO)_n$ series has given rise to numerous studies [6–8]. This series is attractive since different Fe^{III}/Fe^{II} distributions can be expected according to the n member. Some recent works of n=3 member $CaFe_5O_7$ by transmission electron microscopy (TEM) and X-ray diffraction techniques depending on temperature have revealed some complex structural features [7] and a concomitant correlation with the possible charge ordering versus T. Thus beside a superstructure associated to a monoclinic symmetry at room temperature [7], the $CaFe_5O_7$ ferrite exhibits a reversible transition from monoclinic $P2_1/m$ superstructure to orthorhombic *Cmcm* structure at 360 K. That structural transition is associated to a sharp peak in magnetic susceptibility and a clear regime change in resistivity curve [7]. To understand such an interplay between structure and physical properties and the phenomenon that induces this structural transition, a neutron diffraction study combined with some zero-field and in-field ^{57}Fe Mössbauer spectrometry measurements were carried out on $CaFe_5O_7$. This coupled study has given the opportunity to finely analyze the distribution of iron III/II species and follow its evolution and their associated electronic features. Experimental neutron diffraction data were collected at selected temperatures on a large thermal range typically from 5 to 500 K. On the same sample, transmission Mössbauer spectra were recorded at different temperatures and in presence of an external magnetic field at low temperature to better understand the magnetic structure. Owing to this combined approach, three distinct magnetic behaviors are highlighted and described in this paper.

2. Experimental

The $CaFe_5O_7$ sample was synthesized by a standard solid state reaction process using CaO, Fe_2O_3 and Fe as starting materials according to the method previously reported [7]. Purity of the sample

* Corresponding author.

http://dx.doi.org/10.1016/j.jssc.2016.12.021
Received 25 October 2016; Received in revised form 20 December 2016; Accepted 21 December 2016
Available online 22 December 2016

was checked by analyzing powder X-ray diffraction (XRPD) pattern collected with an Xpert Pro Panalytical diffractometer working with the Co Kα radiation and equipped with an X'Celerator detector. Neutron Powder diffraction (NPD) data were collected on the D2B diffractometer at the ILL (Institut Laue Langevin) reactor using two wavelengths: λ=1.594 Å and 2.40 Å. Sample was put in cylindrical vanadium can. Low temperatures data were collected using He_{liq} Cryostat whereas a furnace has been installed for room and higher temperature data collections. All neutron diffraction data collections have been performed under dynamic vacuum. Atomic resolution STEM-HAADF study has been carried out on JEOL ARM200 FEG microscope equipped with aberration correctors.

^{57}Fe Mössbauer spectra were collected using a conventional constant acceleration transmission spectrometer with a ^{57}Co(Rh) source and a bath cryostat for low temperature and a home-made cryofurnace for high temperature. In addition, in-field Mössbauer spectra were collected at different temperatures using a cryomagnetic device generating an external magnetic field parallel to the γ-beam. The spectra were fitted by means of the MOSFIT program with either quadrupolar doublets in the paramagnetic range or magnetic sextets in the magnetically ordered state, both composed of Lorentzian lines. Their relative proportions of these Fe species are given from the corresponding absorption areas, assuming thus the same values of their recoilless Lamb-Mössbauer factors. An α-Fe foil was used as calibration sample while the values of isomer shift are quoted relative to that of α-Fe at 300 K. Susceptibility and magnetization were measured from a dc SQUID Quantum Design magnetometer. Zero field heat capacity measurements were carried out from 2 to 400 K using a semi-adiabatic relaxation technique coupled with a 2τ fitting procedure (PPMS, Quantum Design). Note that all characterizations (XRPD, NPD, ^{57}Fe Mössbauer spectrometry and physical analyses) have been performed on crystalline powders prepared from the same $CaFe_5O_7$ batch.

3. Results and discussions

As recently reported, the $CaFe_5O_7$ oxide which the monoclinic structural model is shown in Fig. 1, exhibits two transitions in the thermal magnetic susceptibility curve at T*=125 K and T_N=360 K [7] respectively. The present analysis of whole NPD patterns collected in the large thermal range from 5 K to 500 K is in agreement with these first results since three different data sets can be evidenced as illustrated in Fig. 2: $T > T_N$=360 K, 125 K < T < 360 K and T < T*=125 K respectively. Based on that observation and combining Mössbauer spectrometry measurements in the same thermal range, both the magnetic behavior evolution and the iron species distribution have been tuned according to T* and T_N.

$T > T_N = 360$ K

Fig. S.I.1 shows the neutron-diffraction pattern of $CaFe_5O_7$ recorded at 500 K. According to our previous study [7], the nuclear cell can be described in an orthorhombic *Cmcm* setting at this temperature. In the present case, the observed neutron pattern is well fitted with these structural data, especially the oxygen content has been refined and corresponds perfectly to the one expected. No magnetic contribution is detected during these calculation series. The difference pattern attests of the goodness of the fit, which is confirmed by the conventional reliability factors. All these calculations are summarized in Table 1.

Above 360 K the Mössbauer spectra exhibit a paramagnetic structure as illustrated in Fig. S.I.2 confirming thus that the compound is in the paramagnetic state. However, as listed in Table 2, the values of isomer shift do not correspond strictly to those of Fe^{3+} and Fe^{2+}, but to the presence of Fe ions with delocalized electron. The hyperfine structure has to be decomposed into two quadrupolar components: it is important to emphasize that among both fitting A and B models describing correctly the hyperfine structure versus temperature, only the A model shows clearly a physically realistic meaning. The second solution involving two quadrupolar doublets with rather similar values of isomer shifts gives rise to a decomposition where the distribution Fe^{3+}/Fe^{2+} differ from expected $2Fe^{3+}$:$3Fe^{2+}$. Indeed, the values of isomer shift have to be assigned to intermediate valence states estimated at about $2.68(5)^+$ and $2.17(5)^+$ respectively; in addition, the monotonic increase of the paramagnetic splitting values with the decreasing temperature up to 360 K suggests also weak changes in the Fe probe atomic neighboring giving rise to a less symmetric environment below T_N=360 K concomitant with the neutron spectra evolution shown in Fig. 2.

$T_N = 360$ K > T > T* = 125 K

Neutron diffraction data shown in Fig. S.I.3 confirms that below T_N the $CaFe_5O_7$ oxide undergoes to a structural transition from an orthorhombic symmetry (*Cmcm*) to a monoclinic one ($P2_1/m$) like revealed by combining electron microscopy and X-ray diffraction analyses [7]. Nevertheless the a_o doubling observed at RT on electron diffraction patterns and on single crystal X-ray diffraction data, induced by the shifting of Ca rows [6,7], is not detected. This is probably due to the weakness of the extra peaks compared to the background as it was already reported in $HoBaCo_2O_5$ for the charge ordered state [9]. Consequently, calculations have been done with the following cell a=3.05 Å, b=17.97 Å, c=5.25 Å and β=106.99° and the

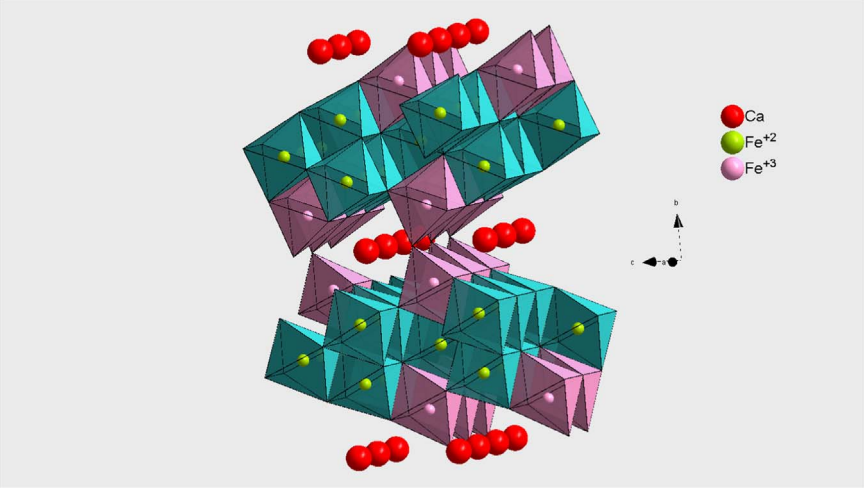

Fig. 1. Structural model of $CaFe_5O_7$ projected along [100] direction. Pink and blue octahedra are related to Fe(III) and Fe(II) species respectively. (For interpretation of the references to color in this figure legend, the reader is referred to the web version of this article.

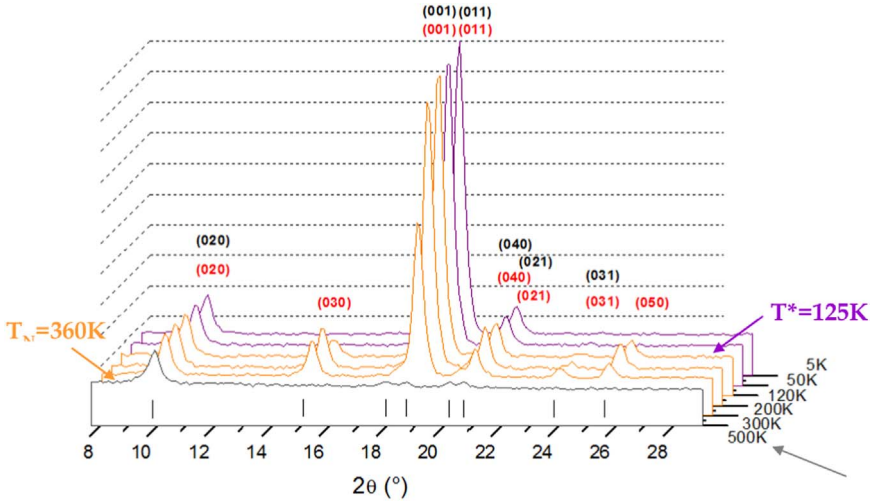

Fig. 2. Thermal Nuclear reflections are reported in black and magnetic reflections in red evolution of the neutron powder diffraction patterns in the range of 5–500 K. (For interpretation of the references to color in this figure legend, the reader is referred to the web version of this article.

Table 1
Refined structure parameters of $CaFe_5O_7$ at 500 K.

Atome	Ox.	Site	x	y	z	Occ.	U_{iso} (Å^2)	BVS
Ca1	+2	4c	0	0.7865(5)	1/4	0.25	0.015(1)	2.00(1)
Fe1	+2	8f	0	0.2746(2)	0.0746(1)	0.5	0.0131(3)	2.09(1)
Fe2	+2	4a	0	0	0	0.25	0.0110(5)	2.07(1)
Fe3	+3	8f	0	0.4630(2)	0.8463(1)	0.5	0.0124(3)	2.31(1)
O1	−2	4c	0	0.4598(5)	1/4	0.25	0.0131(7)	2.14(1)
O2	−2	8f	0	0.9149(4)	0.3920(2)	0.5	0.0172(6)	1.73(1)
O3	−2	8f	0	0.1728(3)	0.3317(1)	0.5	0.0121(5)	2.01(1)
O4	−2	8f	0	0.6371(4)	0.4690(2)	0.5	0.0149(6)	1.62(1)

SG: *Cmcm* a_o=3.0408(1) Å, b_o=10.0769(5) Å, c_o=18.0144(2) Å R_{Bragg}=3.73% R_{wp}=2.83% χ^2=5.74.

Table 2
Refined values of Isomer shifts, mean isomer shift, line width at half height, quadrupolar splitting and relative absorption area estimated from Mössbauer spectra recorded at different temperatures.

T (K)	Model	$\delta_{/Fe\alpha}$ (mm/s) ± 0.01	< δ > (mm/s) ± 0.01	Γ (mm/s) ± 0.02	Δ (mm/s) ± 0.02	Relative absorption area (%) ± 1
373	A	0.54	0.70	0.32	0.84	40
		0.81		0.36	0.66	60
	B	0.64	0.70	0.29	1.07	35
		0.74		0.38	0.52	65
473	A	0.48	0.64	0.31	0.77	41
		0.75		0.32	0.55	59
	B	0.57	0.64	0.26	0.96	34
		0.68		0.36	0.43	66
573	A	0.41	0.56	0.29	0.70	41
		0.67		0.29	0.46	59
	B	0.49	0.57	0.25	0.86	35
		0.61		0.34	0.35	65
665	A	0.35	0.50	0.27	0.63	40
		0.60		0.29	0.38	60
	B	0.42	0.50	0.25	0.78	36
		0.55		0.31	0.28	64

$P2_1/m$ space group which leads to an average structural model where the shifting of calcium atoms inside the channels cannot be highlighted. Three independent iron positions are refined (Table 3) – taking into account the previous results [6–8] the Fe^{3+} species are distributed over the site surrounding the calcium atoms, while the Fe^{2+} atoms sit inside the FeO belt. It is clearly observed that the environments of the iron III ions are more distorted than the other one. Like previously shown in Fig. 2, extra peaks due to magnetic contribution are clearly visible (red indexation). At room temperature, these magnetic Bragg peaks can all be indexed with a propagation vector k=0. After checking the 4 possible magnetic modes obtained with the SaRah software [10], the best agreement with the experimental data was obtained for the magnetic structure given by the basis vectors of the irreducible representation Γ_1 (Table 4). The magnetic moments of Fe atoms order antiferromagnetically in the bc plane (Fig. 3) through the antiferromagnetic super exchange interactions: $Fe^{2+}-O-Fe^{2+}$; $Fe^{3+}-O-Fe^{2+}$ and $Fe^{3+}-O-Fe^{3+}$(θ=90° and 180°). Thus the overall results in "ferromagnetic sheet".

Fig. S.I.4 compares some Mössbauer spectra recorded in the same temperature range, i.e. at 190 and 300 K successively: they consist of the superimposition of magnetic sextets which have to be deconvoluted into at least four different components. In addition a small quadrupolar doublet assigned to FeO structure detected as extended defects inside the $CaFe_5O_7$ matrix [7] must be introduced (green curve in S.I.4). This feature allows the existence of four different Fe magnetic moments to be concluded. The values of isomer shift are respectively plotted versus temperature in Fig. 4a: one should unambiguously attribute the present magnetic sextets to HS Fe^{3+} and HS Fe^{2+} species, contrarily to the paramagnetic temperature range, as aforementioned. The proportions of each Fe species are consistent with the ratio $2Fe^{3+}$:$3Fe^{2+}$ and are in agreement with crystallographic analyses and chemical expectations [6–8]. To better understand the Fe magnetic moments arrangement, we performed in-field Mössbauer spectrometry. When applying an external magnetic field of 8 T at 190 K, the hyperfine structure should be also decomposed into four magnetic sextets, as illustrated in Fig. 4b. The main changes are due to the intensities of the intermediate lines: indeed, they significantly increase in the case of the sextets assigned to the Fe^{3+} species, in agreement with a perpendicular orientation of magnetic moments in respect to the ɣ-beam, i.e. external magnetic field. In the case of Fe^{2+} magnetic moments, one does conclude to a strong canting of Fe magnetic moments in respect to the external field orientation (about 65°). The values of isomer shift and of the respective proportions of Fe species are found similar to those estimated out of external magnetic field. It is also important to emphasize that the mean isomer shift value at high temperature (above 360 K) is consistent with those estimated at lower temperature (Fig. 4a). The proportions of the two components remain rather temperature independent and fairly agree with those established from the neutron diffractions study.

We can note that the overall component of the resultant vectors is not null leading to in-plane canted antiferromagnetic behavior

Table 3
Refined structure parameters of $CaFe_5O_7$ at 300 K (a) and *5 K (b)*.

Atome	Ox.	Site	x	y	z	Occ.	U_{iso}(Å^2)	BVS
Ca1	+2	2e	0.803(4)	1/4	0.5744(2)	0.5	0.012(2)	2.08(3)
Fe1	+2	4f	0.272(2)	0.4251(2)	0.5469(6)	1	0.0089(6)	2.22(2)
Fe2	+3	4f	0.459(2)	0.6538(2)	0.9266(6)	1	0.0075(5)	2.25(2)
Fe3	+2	2a	0	1/2	0	0.5	0.0052(8)	2.03(1)
O1	−2	2e	0.462(4)	1/4	0.911(2)	0.5	0.007(1)	2.20(3)
O2	−2	4f	0.900(3)	0.1069(2)	0.825(1)	1	0.015(1)	1.74(2)
O3	−2	4f	0.631(3)	0.0316(2)	0.280(1)	1	0.0076(8)	1.64(2)
O4	−2	4f	0.176(3)	0.1674(2)	0.348(1)	1	0.0073(9)	2.05(2)
SG: $P2_1/m$ a_m=3.0454(1) Å, b_m=17.9659(3) Å, c_m=5.2482(1) Å, β=107.012(1)°, T=300 K, R_{Bragg}=4.90%, R_{wp}=4.13%, χ^2=8.08								
Atome	**Ox.**	**Site**	**x**	**y**	**z**	**Occ.**	**U_{iso}(Å^2)**	**BVS**
Ca1	+2	2e	0.784 (3)	1/4	0.5715(1)	0.5	0.014(1)	2.28(2)
Fe1	+2	4f	0.2742(9)	0.4248(1)	0.5480(5)	1	0.0036(4)	2.26(1)
Fe2	+3	4f	0.4704(9)	0.6537(1)	0.9257(5)	1	0.0044(3)	2.25(1)
Fe3	+2	2a	0	1/2	0	0.5	0.0025(6)	2.02(1)
O1	−2	2e	0.452(2)	1/4	0.9144(1)	0.5	0.0081(9)	2.10(2)
O2	−2	4f	0.9051(2)	0.1065(2)	0.8243(1)	1	0.0184(8)	1.80(1)
O3	−2	4f	0.6607(2)	0.0318(2)	0.2836(9)	1	0.0081(6)	1.80(1)
O4	−2	4f	0.1810(1)	0.1682(2)	0.3500(8)	1	0.0061(6)	2.02(1)
SG: $P2_1/m$ a_m=3.0443(1) Å, b_m=17.9071(2) Å, c_m=5.2325(1) Å, β=106.53(1)°, T=5 K, R_{Bragg}=4.43%, R_{wp}=3.36%, χ^2=8.55.								

Table 4
Basis vectors for the space group $P2_1/m$ with k=(0,0,0). The decomposition of the magnetic representation for the Fe1 and Fe2 sites is $\Gamma_{mag} = 3\Gamma_1^1 + 3\Gamma_2^1 + 3\Gamma_3^1 + 3\Gamma_4^1$. The atoms are defined according to 1:(*x,y,z*), 2:(*-x,1/2+y,-z*), 3:(*-x,-y,-z*) and 4:(*x,1/2-y,z*). For the Fe3 site, $\Gamma_{mag} = 3\Gamma_1^1 + 0\Gamma_2^1 + 3\Gamma_3^1 + 0\Gamma_4^1$ and the atoms are defined as 1:(0,1/2,0) and 2:(0,0,0).

Atom	Ψ_1	Ψ_2 (□1)	Ψ_3	Ψ_4	Ψ_5 (□2)	Ψ_6	Ψ_7	Ψ_8 (□3)	Ψ_9	Ψ_{10}	Ψ_{11} (□4)	Ψ_{12}
	$m_{//a}$	$m_{//b}$	$m_{//c}$	$m_{//a}$	$m_{//b}$	$m_{//c}$	$m_{//a}$	$m_{//b}$	$m_{//c}$	$m_{//a}$	$m_{//b}$	$m_{//c}$
m_1	1	1	1	1	1	1	1	1	1	1	1	1
m_2	−1	1	−1	−1	1	−1	1	−1	1	1	−1	1
m_3	1	1	1	−1	−1	−1	1	1	1	−1	−1	−1
m_4	−1	1	−1	1	−1	1	1	−1	1	−1	1	−1

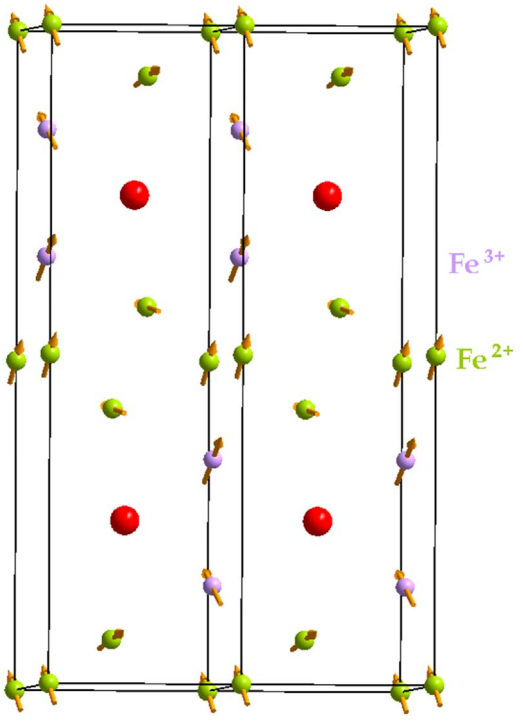

Fig. 3. Magnetic structure projection of $CaFe_5O_7$ at 300 K.

(Table 5). By decreasing the temperature, a change occurs in the magnetic structure around 125 K, illustrated by a rapid decrease of the intensity of the *0k0 k* odd peaks from 125 K until their extinction below 80 K (Fig. 2).

T < T* = 125 K

So far, no change has been observed in the actual monoclinic symmetry ($P2_1/m$) between 300 K and 5 K as summarized in Table 3a–b. However, in the same way as the clear transition at T_N=360 K, a distinct shoulder at T*=125 K is noticed in the thermal evolution of the cell volume (Fig. 5) mainly due to a change in the *a* cell parameter. This transition also affects lightly the Fe-O distances at the level of basal planes (Fig. S.I.5).

At 5 K, the irreducible representation Γ_1 does not fit anymore and the Γ_3 representation is required to obtain a good adjustment as illustrated by the final plot difference shown in Fig. S.I.6. The magnetic moments of Fe atoms still order with the same antiferromagnetic structure but with an orientation of the moment exclusively along b (Fig. 6). We can notice that a similar feature is reported in α-Fe_2O_3 hematite structure [11]. In the latter, this spin-flop transition – well known as the Morin transition- is associated to an antiferromagnetic ordering that is reorganized from being aligned perpendicular to the c-axis to be aligned parallel to the c-axis below T_M=260 K. As for Γ_1, values of the magnetic moments are smaller than that expected for the irreducible representation Γ_3 (Table 5) but in that case magnitude of the resultant component is null.

The Mössbauer spectra characteristics of this temperature range are illustrated in Fig. 7. In Fig. 7a, one observes a progressive collapse of outermost lines corresponding to the Fe^{3+} magnetic sextet, which is completely achieved at both 110 and 77 K, as it is shown in Fig. 7b, while the second component assigned to the Fe^{2+} magnetic sextet remains rather complex independently on the temperature. Indeed, it is necessary to use 2 sub-components to well describe the Fe^{3+} contribution but several sub-components have to be considered in the case of the Fe^{2+} contribution. In addition to model those spectra, the FeO contribution was not considered because its hyperfine magnetic structure which is strongly dependent on the stoichiometry

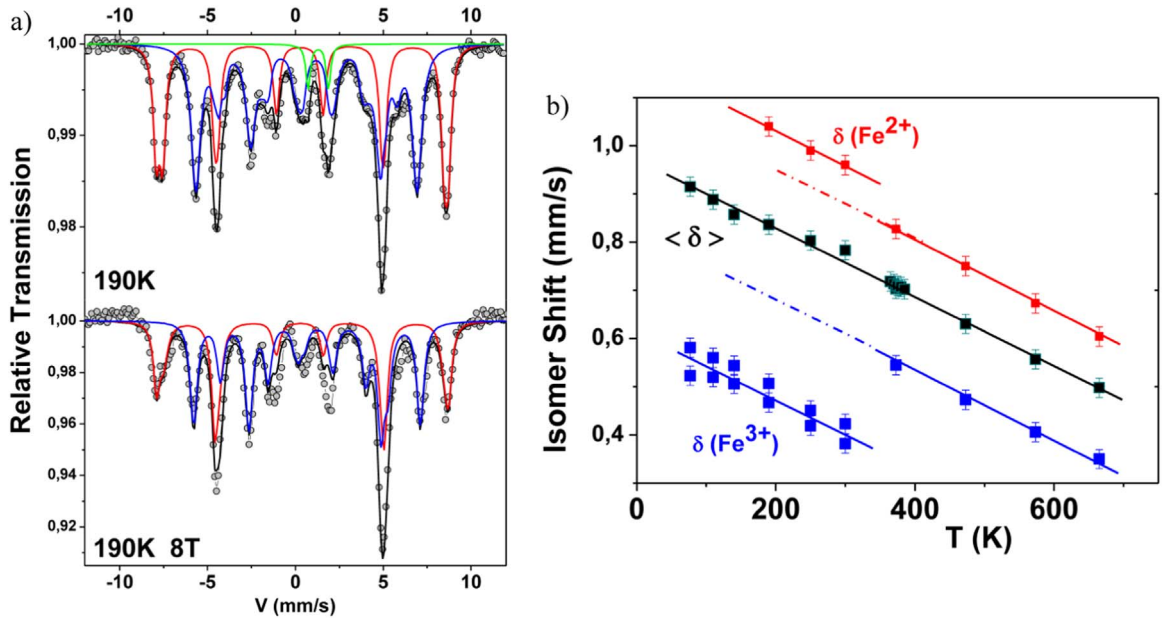

Fig. 4. (a). Isomer shifts depending on temperature deduced from Mössbauer spectra. Fe^{3+} and Fe^{2+} magnetic sextet contributions are red- and blue-colored, respectively. Spectra collected at 190 K without and under an 8 T external magnetic field are shown in (b). (For interpretation of the references to color in this figure legend, the reader is referred to the web version of this article.)

Table 5
Directions and components of magnetic moments of $CaFe_5O_7$ at room temperature and 5 K.

		m_x		m_y		m_z		m_{tot}	
Site	**Ox**	**300 K**	**5 K**	**300 K**	**5 K**	**300 K**	**5 K**	**300 K**	**5 K**
Fe1	+2	−2.9	0	0.4	−3.8	−0.30	0	2.80	3.8
Fe2	+3	3.3	0	0.8	3.9	0.50	0	3.20	3.9
Fe3	+2	1.8	0	0.9	3.5	0	0	2.0	3.5

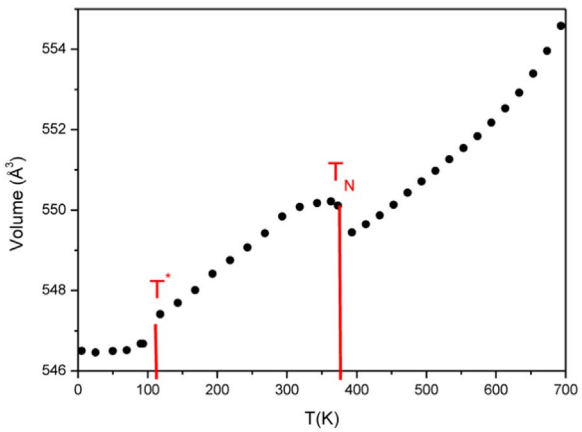

Fig. 5. (a) Thermal dependence of unit cell volume of $CaFe_5O_7$.

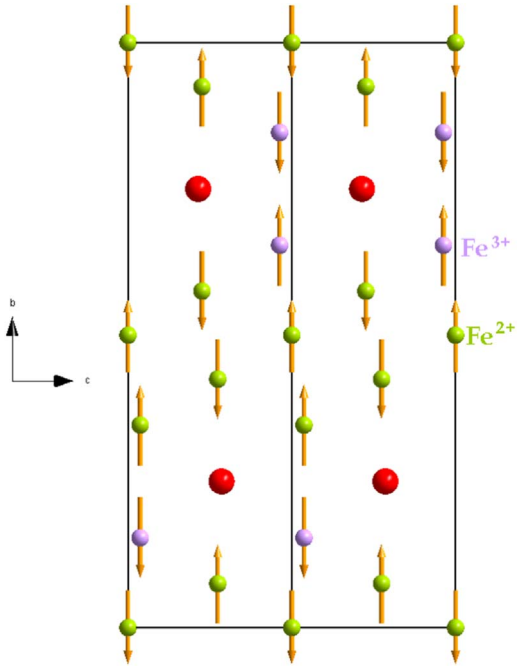

Fig. 6. Magnetic structure projection of $CaFe_5O_7$ at 5 K.

cannot be *a priori* established and its content remains very small (< 5%) compared to the main phase. The fitting model is not unique but the different ones give rise to similar mean values of the different pertinent hyperfine parameters. It is important to emphasize that the more significant change between the two pre-defined temperature domains is due to that of the quadrupole shift of one ferric species: above 125 K, their values rather temperature independent are about +0.20 mm/s while they are about 0.20 and −0.20 mm/s below 125 K for the two ferric iron species. Such a sharp change which is also observed in the case of hematite (α-Fe_2O_3) and such a difference is consistent with a rotation of the electric field gradient (EFG) principal axis: it should result from a rotation of Fe magnetic moments, as it occurs in the case of hematite at the Morin transition [12–14]. Indeed, this transition is associated to a Fe magnetic moment rotation inducing a pure antiferromagnetic behavior below 125 K into a weak ferromagnetic structure above 125 K with parallel and perpendicular orientation with respect to the c-axis, respectively. Different authors reported that this transition occurs in well-crystallized hematite samples and disappears for poor-crystallized ones [15].

In the case of present $CaFe_5O_7$ ferrite, it is clear that this change should affect the magnetic configuration of both Fe species, but especially that of the Fe^{2+} magnetic network, contrarily to hematite which consists of a single Fe^{3+} species. To check such a behavior, we performed an in-field Mössbauer spectrum at 8 K (which has to be rather similar to that at

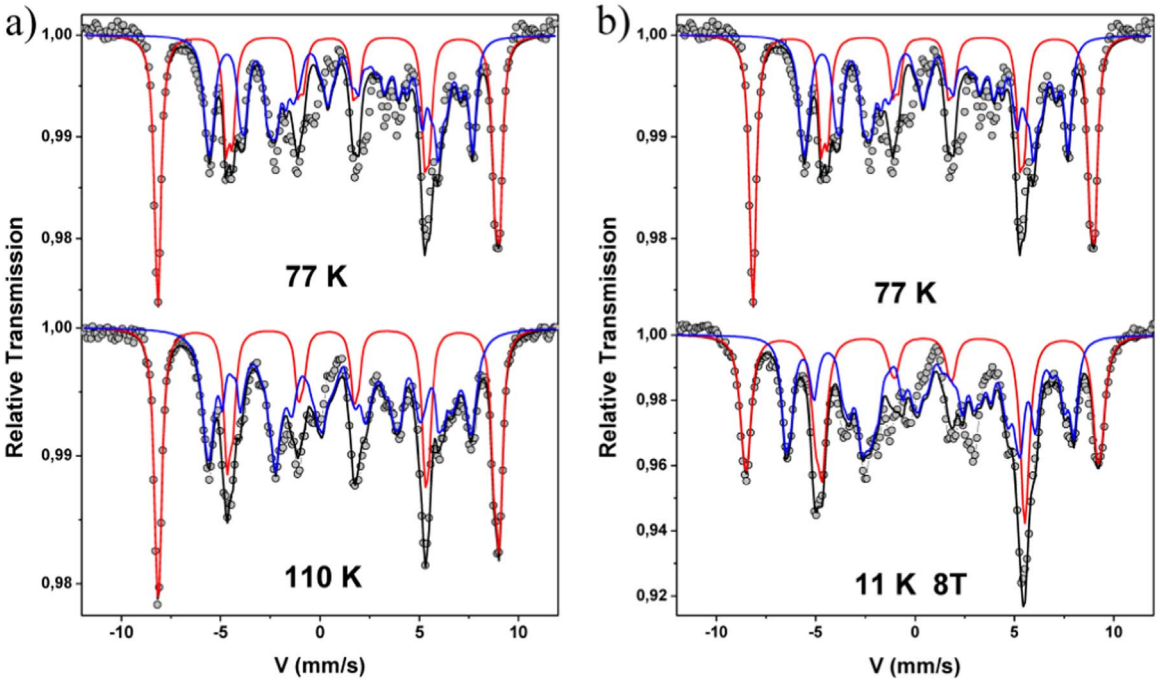

Fig. 7. Mössbauer spectra recorded at 77 K and 110 K on $CaFe_5O_7$ without field (a) and under an 8 T external magnetic field at 77 K and 11 K (b). Fe^{3+} and Fe^{2+} magnetic sextet contributions are red- and blue-colored, respectively. (For interpretation of the references to color in this figure legend, the reader is referred to the web version of this article.)

77 K). Figs. 4b and 7b compare zero-field and in-field 8 T Mössbauer spectra recorded above and below 125 K respectively. One observes interesting similarities with the intensity of the intermediate lines corresponding to that of the Fe^{3+} component but significant differences in the profile of the in-field second magnetic component assigned to the Fe^{2+} species. The application of the external field induces a rotation of Fe^{3+} magnetic moments, rather perpendicular to the external field, i.e. to the γ-beam, giving rise to the same in-field magnetic structure as observed in the intermediate temperature range. On the contrary, the magnetic Fe^{2+} hyperfine structure which appears more complex at low temperature with some non-collinear structure rather perpendicular to the external magnetic field, should result from the rotation of Fe^{3+} magnetic moments induced by the external magnetic field, both competing with the strong single-ion anisotropy of Fe^{2+}. In addition, let us remember an additional feature with the presence of Fe^{3+} Mössbauer components as previously discussed originated from some chemical disorder which prevents from a well-defined transition. Those different points make the fitting model quite complex to be established: one does consider that it is not unique but the better physical description involving the minimum number of free parameters, as is shown in Fig. 6, provides hyperfine data which are consistent with those obtained in zero-field conditions at 77 K (the temperature is rather small). Nevertheless, the in-field magnetic configuration of $CaFe_5O_7$ ferrite appears to be fairly consistent with that established from neutron diffraction. The similarity of the low and high temperature in-field magnetic configurations suggests that the external magnetic field acts as the evolution of temperature does.

To better characterize the two transitions T* and T_N, at 125 K and 360 K (Fig. S.I.7) respectively, thermal dependence of the heat capacity of our sample has been collected from 5 K to 400 K (Fig. 8). The T_N transition which comes with a structural transition, clearly implies a huge and sharp peak in the heat capacity, characteristic of a first order transition, while at T* no change can been evidenced. The T* transition marking the change between the magnetic structures $\mathbf{\Gamma_1}$ and $\mathbf{\Gamma_3}$ and resulting from a spin rotation is hardly detectable by Cp owing to a small associated entropy change. Similar conclusions can be made in the case of α-Fe_2O_3 hematite [11] but also in the GdFeO3 orthoferrite [16]. However, the magnetizations curves versus magnetic field, collected at several temperatures in the range from 10 K to 300 K (Fig. 9), show that from

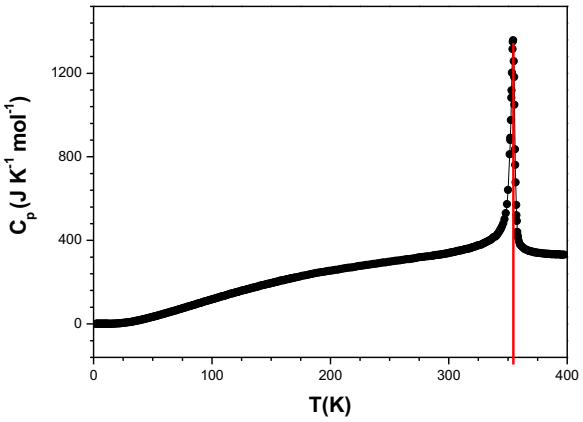

Fig. 8. Zero-field heat capacity curve of $CaFe_5O_7$.

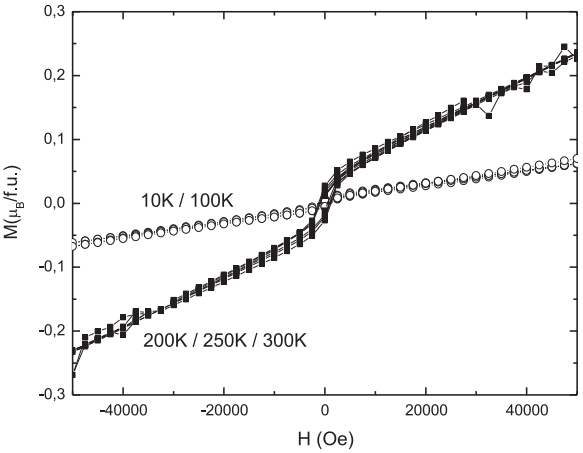

Fig. 9. Magnetization loops above and below T*=125 K.

either side of T*, two magnetic behaviors can be definitely distinguished. Above T*=125 K, in agreement with our neutrons diffraction data studies, a canted antiferromagnetic behavior induces a hysteresis (H_c=0.1 T) with significant values of magnetization but without reaching any saturation. Below T*, values of magnetizations are lower and no hysteresis is observed which is in agreement with the alignment of the moment along the b axis. One can notice that T* correspond to a spin canting from the ac plane (above T*) to the b axis (below T*) which must correspond to the magnetic easy axis.

4. Concluding remarks

This paper reports on the magnetic behavior of $CaFe_5O_7$ from 4 to 500 K. Three distinct magnetic domains around T*=125 K and T_N=360 K are highlighted. By analogy with the T_M=260 K spin-flop transition reported in α-Fe_2O_3 hematite structure [11] T* can be assigned to T_M. Even if magnetic measurements have been performed from powder sample, the corresponding neutron analyses evidence clearly a magnetic anisotropy for our compound. This effect is the consequence of a competition between the magnetic anisotropy of the Fe layers (ac plane) and the inter layer coupling favoring a collinear alignment along b. The present Mössbauer study combining zero-field and in-field experiments nicely confirms that a magnetic phase transition, so-called Morin transition, occurs at T_M=125 K in $CaFe_5O_7$ ferrite with a reorientation of Fe^{3+} magnetic moment. A more quantitative and detailed description would require a systematic Mössbauer study performed at 11 K and 190 K versus the external magnetic field, as the present ferrite exhibits a more complex structural and magnetic structure than that of hematite. Also these results encourage us to prospect other members of the intergrowth $(CaFe_2O_4)(FeO)_n$ series to study the impact of Fe^{2+}/Fe^{3+} distribution on these transitions.

Acknowledgements

The authors acknowledge the financial support of the French Agence Nationale de la Recherche (ANR), through the program “Investissements d′Avenir” (ANR-10-LABX-09-01), LabEx EMC^3.

The authors thank to F. Veillon for technical support in physical measurements.

Appendix A. Supplementary material

Supplementary data associated with this article can be found in the online version at http://dx.doi.org/10.1016/j.jssc.2016.12.021.

References

[1] H. Fjellvag, F. Gronvold, S. Stolen, On the crystallographic and magnetic structures of nearly stoichiometric iron monoxide, J. Solid State Chem. 124 (1996) 52.
[2] R.C. Pullar, Hexagonal ferrites: a review of the synthesis, properties and applications of hexaferrite ceramics, Prog. Mater. Sci. 57 (2012) 1191.
[3] N. Hollmann, M. Valldor, Hua Wu, Z. Hu, N. Qureshi, T. Willers, Y.-Y. Chin, J.C. Cezar, A. Tanaka, N.B. Brookes, L.H. Tjeng, Orbital occupation and magnetism of tetrahedrally coordinated iron in CaBaFe4O7, Phys. Rev. B 83 (2011) R180405.
[4] E.J.W. Verwey, Electronic conduction of magnetite (Fe_3O_4) and its transition point at low temperatures, Nature 144 (1939) 327.
[5] J. Garcia, G. Subias, The Verwey transition – a new perspective, J. Phys., Condens. Matter 16 (2004) R145.
[6] C. Delacotte, F. Hüe, Y. Bréard, D. Pelloquin, Transmission electron microscopy study of CaFe5O7: evidence of a monoclinic superstructure at room temperature, Key Eng. Mater. 617 (2014) 237.
[7] C. Delacotte, F. Hüe, Y. Bréard, S. Hébert, O. Pérez, V. Caignaert, J.M. Greneche, D. Pelloquin, Structural transition at 360 K in the $CaFe_5O_7$ ferrite: toward a new charge ordering distribution, Inorg. Chem. 53 (2014) 10171.
[8] O. Evrard, B. Malaman, F. Jeannot, A. Courtois, H. Alebouyeh, R. Gerardin, Mise en évidence de CaF2e4O6 et détermination des structures cristallines des ferrites de calcium CaFe2+nO4+n (n=1, 2, 3): nouvelle example d′intercroissance, J. Solid State Chem. 35 (1980) 112.
[9] E. Suard, F. Fauth, V. Caignaert, I. Mirebeau, G. Baldinozzi, Charge ordering in the layered Co-based perovskite HoBaCo2O5, Phys. Rev. B 61 (2000) R11871.
[10] A.S. Wills, SARAh software, Physica B 276 (2000) 680–681.
[11] F.J. Morin, Magnetic susceptibility of alpha-Fe_2O_3 and alpha-Fe_2O_3 with added titanium, Phys. Rev. 78 (1950) 819.
[12] F. van der Woude, Mössbauer effect in α-Fe_2O_3, Physica Status Solidi 17 (1966) 417.
[13] N.N. Greenwood, T.C. Gibb, Mössbauer Spectroscopy, Chapman and Hall, 1971 (references therein).
[14] E. Van San, E. De Grave, R.E. Vandenberghe, Field-induced spin transitions in hematite powders as observed from Mossbauer spectroscopy, J. Magn. Magn. Mater. 269 (2004) 54.
[15] R.E. Vandenberghe, E. De Grave P71, Yutaka Yoshida, Guido Langouche (Eds.), Mössbauer Spectroscopy, Springer, Berlin Heidelberg, 2013 (references therein).
[16] G. Gorodetsky, L.M. Levinson, Direct observation of reorientation of antiferromagnetic axis in DyFeO3, Phys. Lett. A 31 (1970) 115.